Compernolle Steven (Orcid ID: 0000-0003-0872-0961)
Stavrakou Trissevgeni (Orcid ID: 0000-0002-2952-8306)
Müller Jean-François (Orcid ID: 0000-0001-5335-2622)
van der A Ronald, J. (Orcid ID: 0000-0002-0077-5338)

Impact of coronavirus outbreak on NO₂ pollution assessed using TROPOMI and OMI observations

M. Bauwens[1], S. Compernolle[1], T. Stavrakou[1], J.-F. Müller[1], J. van Gent[1], H. Eskes[2], P. F. Levelt[2,3], R. van der A[2], J. P. Veefkind[2], J. Vlietinck[1], Huan Yu[1], C. Zehner[4]

[1] Royal Belgian Institute for Space Aeronomy (BIRA-IASB), Avenue Circulaire 3, 1180 Brussels, Belgium

[2] Royal Netherlands Meteorological Institute (KNMI), Utrechtseweg 297, 3731 GA De Bilt, The Netherlands

[3] Delft University of Technology (TU Delft), Department of Geoscience and Remote Sensing, Stevinweg 1, 2628 CN Delft, The Netherlands

[4] ESA/ESRIN, Frascati, Italy

Corresponding author: Trissevgeni Stavrakou (jenny@aeronomie.be)

Key Points:

- Satellite NO₂ data show substantial decreases by 40% on average over Chinese cities due to lockdown measures against the coronavirus outbreak

- Western Europe and U.S. display robust NO₂ decreases in 2020, 20-38% relative to the same period in 2019

- Satellite NO₂ data above Iran, a region strongly affected by coronavirus, does not show clear evidence of lower emissions

Abstract

Spaceborne NO_2 column observations from two high-resolution instruments, TROPOMI onboard Sentinel-5 Precursor and OMI on Aura, reveal unprecedented NO_2 decreases over China, South Korea, Western Europe and the U.S. as a result of public health measures enforced to contain the coronavirus disease outbreak (Covid-19) in January-April 2020. The average NO_2 column drop over all Chinese cities amounts to -40% relative to the same period in 2019, and reaches up to a factor of ~2 at heavily hit cities, e.g. Wuhan, Jinan, while the decreases in Western Europe and the U.S. are also significant (-20 to -38%). In contrast with this, although Iran is also strongly affected by the disease, the observations do not show evidence of lower emissions, reflecting more limited health measures.

1 Introduction

Nitrogen oxides ($NOx=NO_2+NO$) are among the main drivers in air quality degradation in urban/industrialized centers, due to their role as catalysts of tropospheric ozone formation, and as precursors of secondary inorganic aerosols, with consequences for climate and human health (Myhre et al., 2013, Lelieveld et al., 2015, Atkinson et al., 2018). The anthropogenic source of NO_x, primarily originating in fuel combustion accounts for about 65% of the global total NOx emission, the rest being due to emissions from vegetation fires, lightning and soils. Due to their link with human activities, NOx atmospheric levels over cities show a weekly cycle with clear minima during the official rest days in most countries (Beirle et al. 2003); important reductions were also reported during public holidays, like the Chinese New Year (Tan et al. 2009). Due to their adverse health effects, the emissions of NO_x and other pollutants are regulated in many countries. Long-term records of satellite observations of NO_2 columns have been previously used to assess the effectiveness of long-term abatement strategies (Duncan et al., 2015, De Foy et al., 2016, van der A et al., 2017), and the effects of economic recession (Castellanos and Boersma, 2012). Moreover, satellite observations complemented by in situ measurements have been used to determine the impact on air quality of short-term emission regulations during specific events, like the 2008 Olympic Games in Beijing (Mijling et al. 2009, Guo et al. 2013), the 2014 Youth Olympic Games in Nanjing (Ding et al. 2015), the 2010 World Expo in Shanghai (Hao et al. 2011), and the 2014 Asia-Pacific Economic Cooperation summit in Beijing (Huang et al., 2015, Liu et al., 2016).

The ongoing global outbreak of coronavirus disease (Covid-19), declared as a public health emergency of international concern by the World Health Organization (World Health Organization, 2020a), led to unprecedented public health responses in many countries around the world including travel restrictions, curfews, and quarantines. The most drastic and consequential quarantines were those of Hubei province in China (Griffiths and Woodyatt, 2020) and Italy (Horowitz, 2020). Their enforcement, combined with measures in other countries, as well as voluntary limitations of activity (Kim, 2020), result in sweeping disruptions of social and economic activities and even risk of global recession (Leggett, 2020).

In this study, we investigate the impacts of activity reductions resulting from the spread of Covid-19 on NO_2 levels in China, South Korea, Italy, Spain, France, Germany, Iran, and the U.S., all major epicenters of the outbreak. To that aim, we use NO_2 column data from two high-resolution nadir-viewing satellite sensors, the Tropospheric Monitoring Instrument (TROPOMI), single payload of the Sentinel-5 Precursor launched in October 2017 (Veefkind et al., 2012), and the Ozone Monitoring Instrument (OMI, Levelt et al., 2006) launched in 2004

on the Aura platform. Both sensors have an overpass local time of ca. 13:40, and provide daily global coverage at resolutions of 5.5×3.5 km^2 (TROPOMI) and 13×24 km^2 (OMI).

2 Satellite Observations and Processing

The OMI QA4ECV NO$_2$ dataset is based on revised spectral fitting features accounting for improved absorption cross sections, instrument calibration, and surface effects (Boersma et al., 2018, Zara et al., 2018). The data are processed according to the data quality recommendations (Boersma et al., 2017a), and were validated against ground measurements (Compernolle et al., 2020). The TROPOMI NO$_2$ data benefit from the developments of the OMI QA4ECV retrieval (van Geffen et al., 2019a). In this work we use TROPOMI global daily gridded data at 0.05°×0.05° derived from the near-real-time operational product (NRTI, van Geffen et al., 2019a, b), obtained via the Copernicus open data access hub (https://s5phub.copernicus.eu).

To generate time series of NO$_2$ columns over specific locations, we first select pixels from an overpass area, defined by a 100 km radius around the location of interest. For TROPOMI, we use data for which the quality assurance value is higher than 0.5 and the cloud fraction within the NO$_2$ retrieval window is below 40%. For OMI, we follow the recommended quality filter criteria (Boersma et al., 2017b), slightly adapted by Compernolle et al., (2020), as well as the cloud fraction upper limit of 40%. The recommended cloud fraction filtering (Boersma et al., 2018, van Geffen et al., 2019a,b) is actually more strict, but deteriorates the statistics, especially above aerosol-polluted regions. Moreover, focusing only on near-cloud-free scenes could lead to a negative sampling bias (Compernolle et al., 2020) as NO$_2$ polluted scenes tend to be excluded. Per overpass, the remaining pixels are averaged arithmetically 14-day rolling means are calculated and data from 2020 are compared with the previous year (TROPOMI) or the previous 15 years (OMI), in order to distinguish yearly returning patterns (like the Chinese New Year holiday) from the measures taken against the spread of coronavirus, and to link these measures with the observed NO$_2$ levels. The most recent observation date included in this study is 13 April 2020. We have tested an alternative data selection adopting a 50 km radius (instead of 100 km) to assess the robustness of the NO$_2$ reductions.

TROPOMI and OMI single-pixel uncertainties in the winter period are typically ~40-60% of the total column value (value based on Wuhan and Milan overpasses). However, in this work we apply temporal or spatial averaging which will cancel out part of the error (its random component), while the systematic error component is persistent. When we report relative differences between 2019 and 2020, a major part of this systematic error is expected to cancel out.

The systematic absolute difference between TROPOMI and OMI NO$_2$ columns (Figure 2 and S2) stems mainly from the use of different cloud pressure products, O$_2$-O$_2$ cloud retrievals used for OMI (Veefkind et al., 2016), and FRESCO retrievals in the O$_2$-A band used for TROPOMI. In the current implementation of FRESCO O$_2$-A in the TROPOMI processor, the algorithm is found to overestimate the pressure for near-surface clouds or thick aerosol layers. Especially in conditions with moderate to high aerosol pollution levels, the algorithm produces NO$_2$ columns which are on average 10-12% lower than OMI in Europe and the U.S., and up to 20% lower in Eastern China (Eskes et al., 2020). Note, however, that most of this OMI-TROPOMI difference is expected to cancel out when we calculate column ratios between 2019 and 2020.

3 Results

3.1 China

A lockdown was enforced in Wuhan and other cities of the Hubei province on January 23 (Table S1 and Figure S1). On February 2-4, it was extended to several cities in other provinces (Table 1). Analyzing the impacts of the lockdown is complicated by the coincidence of Chinese New Year holidays (24 January – 2 February in 2020) with the initial phase of the Hubei lockdown. The NO_2 reduction during the New Year holiday period is a yearly returning phenomenon (Tan et al., 2009). In addition, NO_2 abundances exhibit a pronounced seasonal cycle (Shah et al., 2020) with highest values during the winter when the NO_x lifetime is longest due to low solar irradiances and low specific humidity.

Figure 1 presents time-averaged NO_2 columns over China over successive periods in 2020 (a-e) and 2019 (f-j), with indication of the Chinese New Year holiday and of the lockdown. In 2019, TROPOMI observations point to a strong decrease in NO_2 columns during the New Year holiday (4-10 February), reflecting mainly lower emissions during that period. The NO_2 columns recover afterwards (11 February - 25 March 2019), but to levels significantly lower compared to the January values, primarily due to NO_x lifetime changes. The seasonality of NO_2 columns at Chinese cities is well illustrated on Figure 2 and Figure S2, displaying the evolution of NO_2 columns over Chinese cities between July 2019 and June 2020, as seen by TROPOMI (upper row) and OMI (lower row). Besides the strong short-term variability (due to a combination of meteorological variability and large random observational errors), the wintertime maximum is evident at all cities, especially when considering the climatological OMI values averaged over 2005-2019 (green line in the lower panel of Figure 2 and Figure S2). For example at Wuhan and Nanjing, the columns decrease by about a factor of two between January and early March.

In 2020, the coincidence of the initial lockdown phase with the New Year holidays (24 January – 2 February) causes a steep drop of NO_2 columns, reaching a factor of 2 or more at most cities (Figure 1b, Figure 2 and Figure S2). After the holidays, however, the strong NO_2 reduction persists for several weeks, after which the columns recover progressively, reflecting the return of economic activities and emissions. As seen on Figure 2, the NO_2 decreases are very sharp in Wuhan and Nanjing. In these two cities where strict lockdowns were enforced, the columns in the lockdown period are not only much lower than during the same period of the previous year, but also lower than in all previous 15 years of OMI observations. According to TROPOMI data, whereas NO_2 levels stagnated in Wuhan until mid-March, they recovered more rapidly in other cities and returned to near-global levels in early April. Similar behavior is found at most other Chinese cities like Shenzhen, Qingdao, Zhengzhou and Xian (Figure S2).

A quantitative estimate of the impact of the lockdown on NO_2 columns at Chinese cities is given in Table 1. To eliminate the interference of seasonal variation and New Year holidays, the average NO_2 column between 11 February and 24 March 2020 is compared to the average column in the same period in 2019. The average NO_2 drop calculated over Chinese cities affected by the lockdown amounts to -40% according to both TROPOMI and OMI (Table 1), and to -45% when the smaller (50 km) radius is adopted for calculating the averages (Figure S3). Stronger reductions of up to -60% are found at the most affected cities, including Wuhan and Xi'an (Figure S3). The decrease is lower for many cities not strongly affected by the lockdown e.g. Beijing (-25 to -40%).

These reductions are comparable with those observed as consequence of temporary stringent emission regulations, e.g. in Beijing during the APEC Blue event in November 2014 (-21%) and Parade Blue in August 2015 (-43%) (Liu et al., 2016), and with the column reduction reported during the 2008 Olympic Games in Beijing (-46%, Mijling et al., 2009).

The observed column decreases are due to the decline of traffic emissions, by far the dominant NOx emission source in cities, as well as to decreases in industrial activities and power generation. A significant drop (-50%) in coal-fired power generation was recorded in the 10 days following the Chinese New Year in 2020 compared to 2019 (Myllyvirta, 2020). This decline was prolonged for 40 days after the New Year and a clear rebound was reported afterwards (Figure S4). Substantial decreases were also recorded in industrial activity indicators (e.g. steel production, oil refineries). Moreover, air traffic in China dropped in mid-February by 80% compared to January 2020, and showed a small recovery in the beginning of March, although still 61% lower than in January (Zara, 2020).

3.2 Western Europe

In Italy, the outbreak of Covid-19 led first to the quarantine of 11 small towns in Lombardy, close to Milan, and in the Veneto province, starting on 23 February. On 4 March, the government ordered the nationwide lockdown of schools and universities. As in the case of China, the analysis has to take into account the (photochemically-induced) seasonal variation of NO_2 columns and the near-coincidence of the first lockdown with an important holiday, the Carnival, which took place on 24-25 January 2020 (Table S1). As seen on panels e-h of Figure 3, seasonal variations and the Carnival of 2019 might explain (part of) the decline of NO_2 columns measured by TROPOMI over Northern Italy in early March 2019, although synoptic meteorological variability might also contribute.

In 2020, a substantial reduction of NO_x emissions is apparent in the last week of February, especially in Lombardy and Veneto (comparing panels a and b in Figure 3). This reduction, much larger than the corresponding decline in 2019 (panels e-f), is likely mainly due to lower economic activities in response to both the Carnival holidays and the initial measures taken to counter the coronavirus. In March-April, the columns remain very low, not only in comparison with the pre-lockdown values (comparing panels c and d with a), but also compared to the corresponding period in 2019 (g- and -h). The NO_2 levels are unusually low not only in Lombardy and Veneto, but also elsewhere in Italy, e.g. above Turin and Bologna. The average TROPOMI NO_2 column during the lockdown period in 2020 is found to be between 38(±10)% and 33(±9)% lower than during the same period in 2019 in Milan and Venice (Table 1). Those reductions outweigh the combined effect of emission regulations and economic recession on OMI NO_2 columns in Europe over 2004-2010, which was estimated at 20% (Castellanos and Boersma, 2012).

In response to the Covid-19 infection, other European countries declared a state of emergency and placed their countries under lockdown and stay-at-home orders (Table S1). Spain became the most affected country in Europe in number of cases, followed by Italy, France and Germany (as of 25 April 2020), and lockdown measures were enacted in these countries on March 14, 17 and 22, respectively. As a result of these measures, a marked NO_2 column drop (-30%) was observed during the strict lockdowns in Spain and France in comparison with the same period in 2019, whereas more moderate decreases were found in Germany and Belgium (-20%), possibly because the lockdown conditions were less strict in these countries (Figure S5). The average NO_2 decrease over the European cities of Table 1 is very similar between TROPOMI (-27%) and OMI (-25%).

3.3 South Korea

South Korea has been severely affected by the outbreak, although containment measures in these countries were much more limited than in Chinese areas affected by the coronavirus (Table S1). A reduction of economic activities and traffic is nevertheless expected and should be reflected in the satellite NO_2 measurements. Although the first reports of Covid-19 in South

Korea appeared on 20 January 2020 (World Health Organization, 2020b), the South Korean government declared the highest level of health alert on 23 February and asked to refrain from unnecessary travel. While these measures are mostly on a voluntary basis, they clearly led to emission reduction over South Korean cities such as Seoul and Daegu, where the average NO_2 columns during the three first weeks after the reference date (health alert on February 23) are between -43(±7)% (Seoul) and -24(±10)% (Daegu) lower than during the same period one year earlier, based on TROPOMI measurements (Table 1 and Figure S6). It is however not excluded that a small fraction of the reduction could be due to meteorological variability (wind, cloud cover, humidity) which can affect the transport and lifetime of NO_x. Substantial column reductions during these four weeks in 2020 (relative to 2019) are also evident at other large cities including Gwangju (southwest) and Cheongju (center), although not at Busan (south), the second-largest city (Figure S6). The reduction is also clear when comparing the columns on the weeks before and after the lockdown (comparing panels a and b in Figure S6). The columns appeared however to recover in late March and early April (panel c), at least in the Seoul and Daegu areas.

3.4 Iran

Reports that the virus had reached Iran occurred on 20 February 2020 (World Health Organization, 2020c). Although the Iranian government has ordered the closure of schools and universities on 23 February, and imposed a limit on public gatherings on 3 March, these measures are not clearly reflected in the observed NO_2 signal. Compared to the previous year, the average NO_2 levels in Tehran and Isfahan were higher in the first weeks after the reference date (23 February) (Table 1). The temporal evolution of the columns over Tehran, the capital city and strongest NO_2 hotspot (Figure S7) does not indicate significant NO_2 changes in the period before (1-22 February) and after the lockdown (4-20 March). Note that the temporal variability of TROPOMI NO_2 columns over Tehran in wintertime is very strong, reflecting to a large extent the unusually large NO_2 retrieval errors, exceeding 100% over the Tehran agglomeration (Figure S8), although meteorological variability might be an additional contributing factor. A likely explanation for the absence of NO_2 reduction between 4-20 March is that complete lockdowns were not enforced in Iran, as the administration initially ruled out this possibility, while urging people to voluntarily stay at home (Mehdi, 2020). Moreover, Tehran's lockdown was not approved because the government could not provide financial aid to people and businesses. On 28 March, a complete lockdown was imposed (Mehdi, 2020), but stay-at-home calls were largely ignored (Wintour, 2020). The sharp NO_2 column decline from 21 March to 4 April detected in 2019 and 2020 is due to Nowruz, a two-week celebration marking the beginning of the Iranian New Year (Figure S7). Compared to the 3-week period just before the New Year, the columns are reduced by factor of 2-2.5 in Tehran, Isfahan and Qom in 2020.

3.5 U.S.

In March 2020, the focus of the Covid-19 crisis has shifted decisively from Europe to the U.S. which became the next global epicenter of the crisis with the biggest number of confirmed cases in the world (worldometers.info/coronavirus, as of 25 April 2020). In an attempt to slow down the progression of the infection, a large majority of state and local governments responded by declaring emergency and issuing stay-at-home orders, which came into effect at different dates in late March and early April (Secon and Woodward, 2020). Two periods were chosen for the analysis: 23 February-14 March 2020 (pre-lockdown) and 24 March-13 April 2020 with lockdowns in most of the eastern states, e.g. Illinois (21 March), Indiana and Ohio

(23 March), New York (22 March), as summarized in Table S1. In the southeastern states, the lockdowns were enacted in early April and therefore the NO_2 time series are too short to allow robust conclusions. These states were therefore not considered in our analysis. Significant reductions are not only observed over major cities of northeastern U.S., -28(±11)% in New York and -24(±11)% in Philadelphia according to TROPOMI (Table 1), but also in the rural areas where the decreases are often stronger (up to 40%, Figure 4). To a large extent, the decreased NO_2 levels can be attributed to the reported road traffic decline in the U.S. by 42% in 21-27 March, 47% in 28 March-3 April, and 48% in 4-10 April compared to the control week of 22 February 2020 (Schuman, 2020). For a small part, the NO_2 decrease is also explained by emission regulations and their impacts on long-term emission trends, estimated to be of the order of -4%/yr at most between 2005 and 2014 over northeastern U.S. cities (Duncan et al., 2015).

4 Conclusions

Exceptional decreases in NO_2 columns were observed over widespread areas in China, Europe, South Korea and the U.S. in January-April 2020, based on high-resolution spaceborne data. Those decreases are evident not only from the comparison of NO_2 levels before and during the lockdown, but also when contrasting the 2020 levels with those during the same period in 2019. The decreases are mainly attributed to the containment measures against the spread of the Covid-19, which caused sharp reductions in traffic and industrial activities. For a small part, the column reductions could also be due to meteorological variability and to the decline of emissions caused by environmental policy regulations. Model studies will therefore be needed to separate the effects of the enforced health measures from other contributing factors. To this purpose, satellite observations of NO_2 and other compounds (e.g. CO and aerosol optical depth), complemented by in situ observations, will help interpret the observed decreases and assess the full impacts of these measures on air pollution. At the time of drafting, China has lifted most restrictions, while Europe and U.S. are moving towards a prudent loosening of the measures. Further studies will be needed to evaluate the effects of the temporary lockdowns on global air quality and climate, and the gradual return to pre-lockdown periods.

The authors declare no conflicts of interest.

References

Atkinson, R. W., Butland B. K., Anderson H. R. & Maynard, R. L. (2018), Long-term concentrations of nitrogen dioxide and mortality: a meta-analysis of cohort Studies. *Epidemiology (Cambridge, Mass.)*, 29(4), 460–472. doi:10.1097/EDE.0000000000000847

Beirle, S., Platt, U., Wenig, M. & Wagner, T. (2003), Weekly cycle of NO_2 by GOME measurements: a signature of anthropogenic sources. *Atmospheric Chemistry and Physics*, 3, 2225-2232

Boersma, K. F., Eskes, H., Richter, A., De Smedt, I., Lorente, A., Beirle, S., et al. (2017a), QA4ECV NO_2 tropospheric and stratospheric vertical column data from OMI (Version 1.1). Royal Netherlands Meteorological Institute (KNMI). doi:10.21944/qa4ecv-no2-omi-v1.1

Boersma, K. F., van Geffen, J., Eskes, H., van der A, R. J., De Smedt, I., Van Roozendael, et al. (2017b), Product Specification Document for the QA4ECV NO_2 ECV precursor product, QA4ECV Deliverable D4.6, http://www.qa4ecv.eu/sites/default/files/D4.6.pdf, 2017

Boersma, K. F., Heskes, H. J., Richter, A. De Smedt, I., Lorente, A., Beirle, S., et al. (2018), Improving algorithms and uncertainty estimates for satellite NO2 retrievals: results from the quality assurance for the essential climate variables (QA4ECV) project. *Atmospheric Measurement Techniques*, 11, 6651–6678. doi:10.5194/amt-11-6651-2018

Castellanos, P. & Boersma, K. F. (2012), Reductions in nitrogen oxides over Europe driven by environmental policy and economic recession. *Scientific Reports*, 2, 265. doi:10.1038/srep00265

Compernolle, S., Verhoelst, T., Pinardi, G., Granville, J., Hubert, D., Keppens, A., et al. (2020), Validation of Aura-OMI QA4ECV NO_2 Climate Data Records with ground-based DOAS networks: role of measurement and comparison uncertainties. *Atmospheric Chemistry and Physics Discussions*, doi:10.5194/acp-2019-877, in review

De Foy, B., Lu, Z. & Streets, D. G. (2016), Satellite NO_2 retrievals suggest China has exceeded its NOx reduction goals from the twelfth Five-Year Plan. *Scientific Reports*, 6, 35912. doi:10.1038/srep35912

Ding, J., van der A, R. J., Mijling, B., Levelt, P. F. & Hao, N. (2015), NO_x emission estimates during the 2014 Youth Olympic Games in Nanjing. *Atmospheric Chemistry and Physics*, 15(5), 9399–9412. doi:10.5194/acp-15-9399-2015

Duncan, B. N., Lamsal, L.N., Thompson, A.M., Yoshida, Y., Lu, Z., Streets, D. G., et al. (2016), A space-based, high-resolution view of notable changes in urban NO_x pollution around the world (2005-2014), *Journal of Geophysical Research*, 121, 976–996. doi:10.1002/2015JD024121

Eskes, H. J., van Geffen, J., Boersma, K. F. , Sneep, M., ter Linden, M., Richter, A., Beirle, S., and Veefkind, J. P., High spatial resolution nitrogen dioxide tropospheric column observations derived from Sentinel-5P TROPOMI observations. Preprint prepared for *Atmospheric Measurement Techniques* (2020).

Griffiths, J. & Woodyatt, A. (2020), Wuhan coronavirus: Thousands of cases confirmed as China goes into emergency mode. *CNN*. Available from edition.cnn.com/2020/01/26/asia/wuhancoronavirus-update-intl-hnk/index.html (Accessed in 25 April 2020)

Guo, S., Hu, M., Guo, Q., Zhang, X., Schauer, J. J. & Zhang, R. (2013), Quantitative evaluation of emission controls on primary and secondary organic aerosol sources during Beijing 2008 Olympics, *Atmospheric Chemistry and Physics*, 13, 8303–8314. doi:10.5194/acp-13-8303-2013

Hao, N., Valks, P., Loyola, D., Cheng, Y. F. & Zimmer, W. (2011), Space-based measurements of air quality during the World Expo 2010 in Shanghai. *Environmental Research Letters*, 6(4), 044004. doi:10.1088/1748-9326/6/4/044004

Horowitz, J. (2020), Italy Locks Down Much of the Country's North Over the Coronavirus. *The New York Times.* Available from nytimes.com/2020/03/07/world/europe/coro-navirus-italy.html (Accessed in 25 April 2020)

Huang, K., Zhang, X. & Lin, Y. (2015), The 'APEC Blue' phenomenon: Regional emission control effects observed from space. *Atmospheric Research*, 164, 65–75, doi:10.1016/j.atmosres.2015.04.018

Kim, S. (2020), How South Korea lost control of its coronavirus outbreak. *The New Yorker.* Available from newyorker.com/news/news-desk/how-south-korea-lost-control-of-its-coronavirusoutbreak (Accessed in 25 April 2020)

Lelieveld, J., Evans, J. S., Fnais, M., Giannadaki, D. & Pozzer, A. (2015), The contribution of outdoor air pollution sources to premature mortality on a global scale. *Nature*, 525, 367–371

Levelt, P. F., van den Oord, G. H. J., Dobber, M. R., Mälkki, A., Visser, H., de Vries, J., et al. (2006), The Ozone Monitoring Instrument. *IEEE Transactions on Geoscience and Remote Sensing*, 44, No. 5, 1093–1101

Leggett, T. (2020), Coronavirus: Global growth 'could halve' if outbreak intensifies. *BBC*. Available from bbc.com/news/business-51700935 (Accessed in 25 April 2020)

Liu, H., Liu, C., Xie, Z., Li, Y., Huang, X., Wang, S., Xu, J. & Xie, P. (2016), A paradox for air pollution controlling in China revealed by 'APEC Blue' and 'Parade Blue'. *Scientific Reports*, 6, 34408

Mehdi, S. Z (2020), Covid-19: divergent views at top delay lockdown in Iran. Anadolu News Agency. Available from aa.com.tr/en/health/covid-19-divergent-views-at-top-delay-lockdown-in-iran/1782835 (Accessed in 25 April 2020)

Mijling, B., van Der A, R. J., Boersma, K. F., Van Roozendael, M., De Smedt, I., & Kelder, H. M. (2009), Reductions of NO_2 detected from space during the 2008 Beijing Olympic Games. *Geophysical Research Letters*, 36 (13). doi:10.1029/2009GL038943

Myhre, G., Shindell, D., Bréon, F.-M., Collins, W., Fuglestvedt, J., Huang, et al. (2013), Anthropogenic and Natural Radiative Forcing. In: Climate Change 2013: The Physical Science Basis. Contribution of Working Group I to the Fifth Assessment Report of the Intergovernmental Panel on Climate Change. Edited by Stocker, T. F. et al. Cambridge University Press, Cambridge, United Kingdom and New York, NY, USA

Myllyvirta, L. (2020), Analysis: Coronavirus temporarily reduced China's CO_2 emissions by a quarter. *Carbonbrief*. Available from carbonbrief.org/analysis-coronavirus-has-temporarily-reduced-chinas-co2-emissions-by-a-quarter (Accessed in 25 April 2020)

Secon, H. and Woodward, A. About 95% of Americans have been ordered to stay at home. This maps shows which cities and states are under lockdown. *Business Insider*. Available from businessinsider.com/us-map-stay-at-home-orders-lockdowns-2020-3?r=US&IR=T (Accessed in 25 April 2020)

Schuman, R. (2020), INRIX U.S. national Traffic Volume Synopsis. INRIX Fleet. Available from inrix.com/blog/2020/03/covid19-us-traffic-volume-synopsis, inrix.com/blog/2020/04/covid19-us-traffic-volume-synopsis-3, inrix.com/blog/2020/04/covid19-us-traffic-volume-synopsis-4 (Accessed in 25 April 2020)

Shah, V., Jacob, D. J., Li, K., Silvern, R. F., Zhai, S., Liu, M., et al. (2020), Effect of changing NO_x lifetime on the seasonality and long-term trends of satellite-observed tropospheric NO_2 columns over China. *Atmospheric Chemistry and Physics*, 20, 1483–1495, doi:10.5194/acp-2019-670

Tan, P-H., Chou, C., Liang, J.-Y., Chou, C. C.-K. & Shiu, C.-J. (2009), Air pollution 'holiday effect' resulting from the Chinese New Year. *Atmospheric Environment*, 43, 2114–2124, doi: 10.1016/j.atmosenv.2009.01.037

van der A, R. J., Mijling, B., Ding, J., Koukouli, M. E., Liu, F., Li, Q., Mao, H., and Theys, N. (2017), Cleaning up the air: effectiveness of air quality policy for SO_2 and NOx emissions in China. *Atmospheric Chemistry and Physics*, 17, 1775–1789, doi.org/10.5194/acp-17-1775-2017.

van Geffen, J., Eskes, H. J., Boersma, K. F., Maasakkers, J. D. & Veefkind, J. P. (2019a). TROPOMI ATBD of the total and tropospheric NO_2 data products. Royal Netherlands Meteorological Institute, #S5P-KNMI-L2-0005-RP, issue 1.4.0, 6 February 2019

van Geffen, J., Boersma, K. F., Eskes, H., Sneep, M., ter Linden, M., Zara, M. & Veefkind, J. P. (2019b), S5P/TROPOMI NO_2 slant column retrieval: method, stability, uncertainties, and comparisons against OMI. *Atmospheric Measurement Techniques Discussions*, doi:10.5194/amt2019-471, in review

Veefkind, J. P., Aben, I., McMullan, K., Föorster, H., de Vries, J., Otter, G., et al. (2012), TROPOMI on the ESA Sentinel-5 Precursor: A GMES mission for global observations of the

atmospheric composition for climate, air quality and ozone layer applications. *Remote Sensing of Environment*, 120, 70–83. doi:10.1016/j.rse.2011.09.027

Veefkind, J. P., de Haan, J. F., Sneep, M., and Levelt, P. F. (2016), Improvements to the OMI O_2–O_2 operational cloud algorithm and comparisons with ground-based radar–lidar observations. *Atmospheric Measurement Techniques*, 9, 6035–6049, doi:10.5194/amt-9-6035-2016.

Wintour, P. (2020), Iranians ignore requests to stay home for new year celebrations. Available from theguardian.com/world/2020/mar/20/iranian-new-year-self-isolate-covid-19 (Accessed in 25 April 2020)

World Health Organization (2020a), Coronavirus disease (COVID-19) outbreak. Available from who.int/emergencies/diseases/novel-coronavirus-2019 (Accessed in 25 April 2020)

World Health Organization (2020b), Novel Coronavirus (2019-nCoV), Situation report-1, 21 January 2020, who.int/docs/default-source/coronaviruse/situation-reports/20200121-sitrep-1-2019-ncov.pdf

World Health Organization (2020c), Novel Coronavirus (2019-nCoV), Situation report31, 20 February 2020, who.int/docs/default-source/coronaviruse/situation-reports/20200220-sitrep-31-covid-19.pdf (Accessed in 25 April 2020)

Zara, M., Boersma, K. F., De Smedt, I., Richter, A., Peters, E., van Geffen, J., et al. (2018), Improved slant column density retrieval of nitrogen dioxide and formaldehyde for OMI and GOME-2A from QA4ECV: intercomparison, uncertainty characterisation, and trends. *Atmospheric Measurement Techniques*, 11, 4033–4058, doi:10.5194/amt-11-4033-2018

Zara, C. (2020), Watch flight traffic literally disappear from the skies as the coronavirus hits travel demand. Available from fastcompany.com/90473146/watch-flight-traffic-literally-disappear-from-the-skies-as-the-coronavirus-hits-travel-demand (Accessed in 25 April 2020)
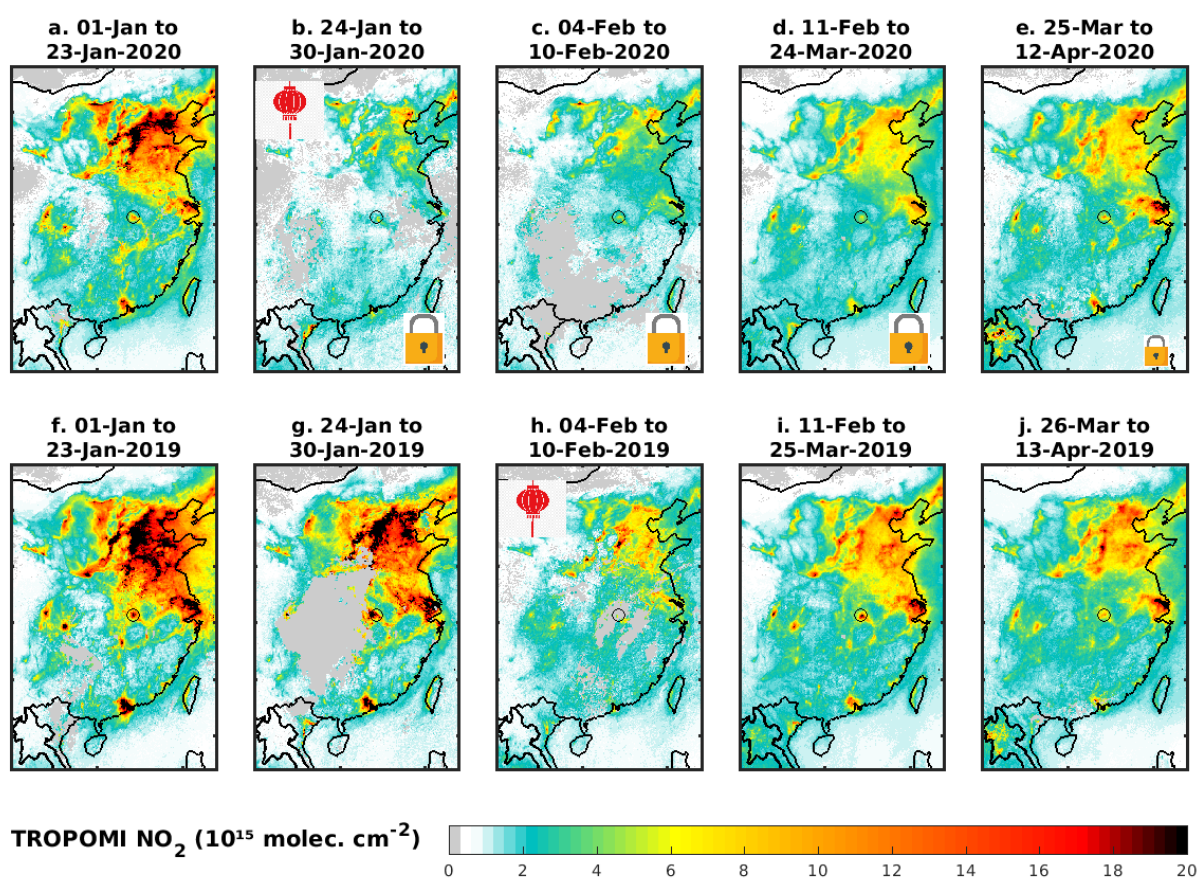
Figure 1. TROPOMI NO₂ columns over China (a) before and (b-e) after the lockdowns (shown by padlocks) due to Covid-19. For comparison, columns over the same time periods are shown for 2019. The week of Chinese New Year holiday is indicated by the red lantern shown inset panels (b) and (h). The New Year holiday covers 4-10 February in 2019, and 24-30 January in 2020 (exceptionally extended to 2 February because of Covid-19). Partial loosening of the restrictions is suggested by the smaller padlock in panel (e). Grey areas indicate no valid data.
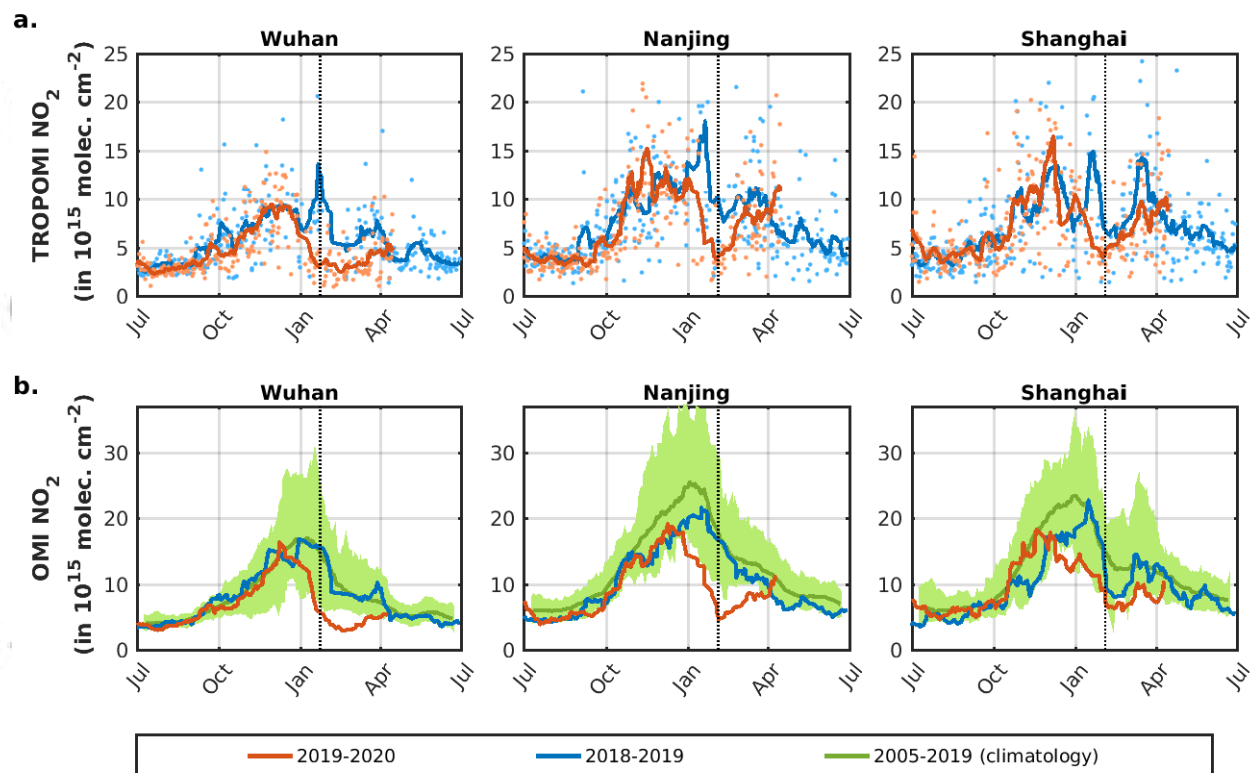
Figure 2. Spaceborne NO$_2$ columns within a 100 km radius around Wuhan, Nanjing and Shanghai (blue symbols for 2018-2019, red symbols for 2019-2020) and 14-day running averages (colored lines). Upper panel: TROPOMI. Lower panel: OMI, including climatological columns (2005-2019) and their range (green).
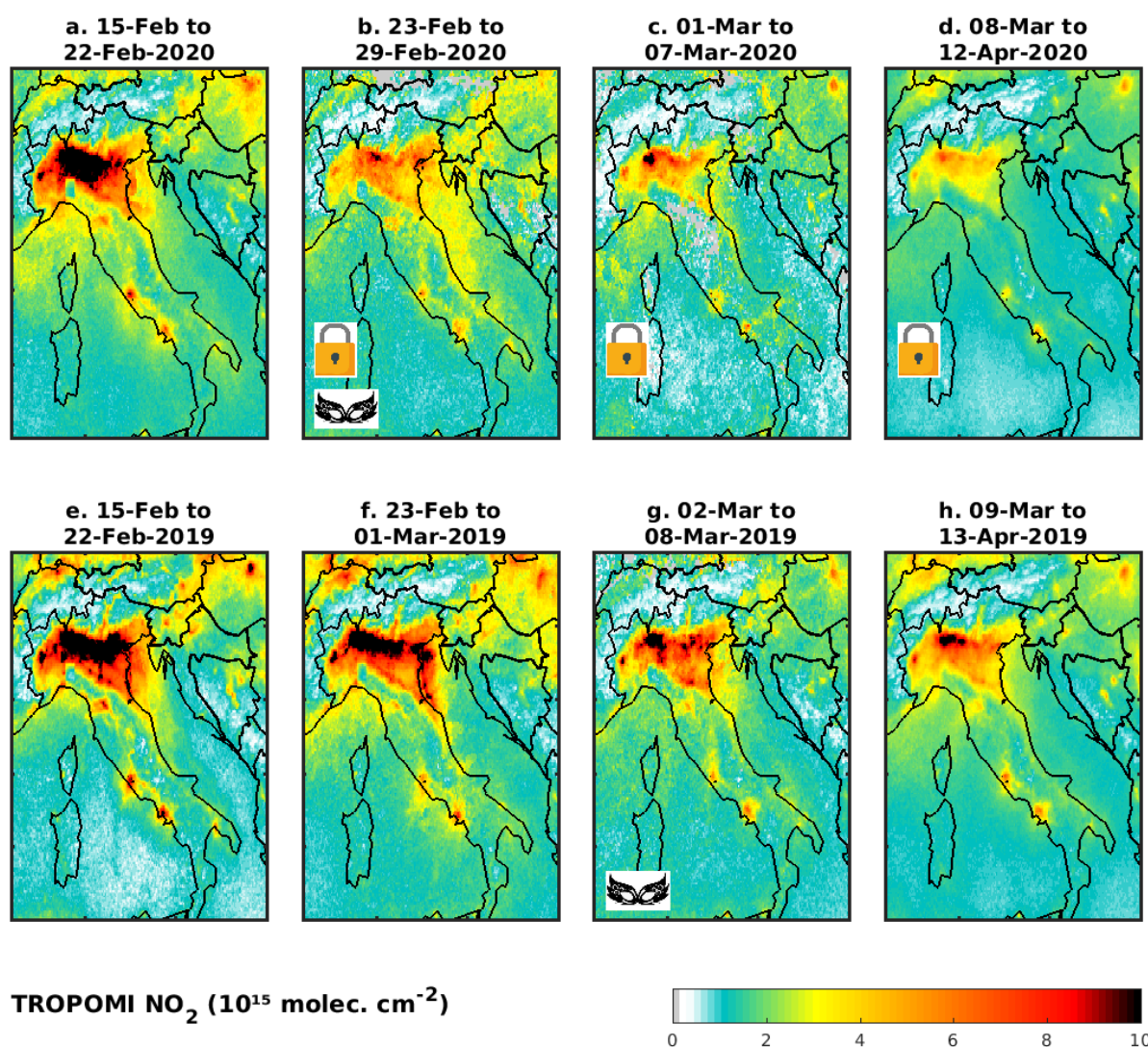
Figure 3. TROPOMI NO$_2$ columns over Italy (a) before and (b-d) during the lockdown in 2020, and over the same time periods for 2019. Note that 2020 is a leap year. The week of Carnival holidays (Table S1) is indicated by masks in panels (b) and (g). Grey areas indicate no valid data.
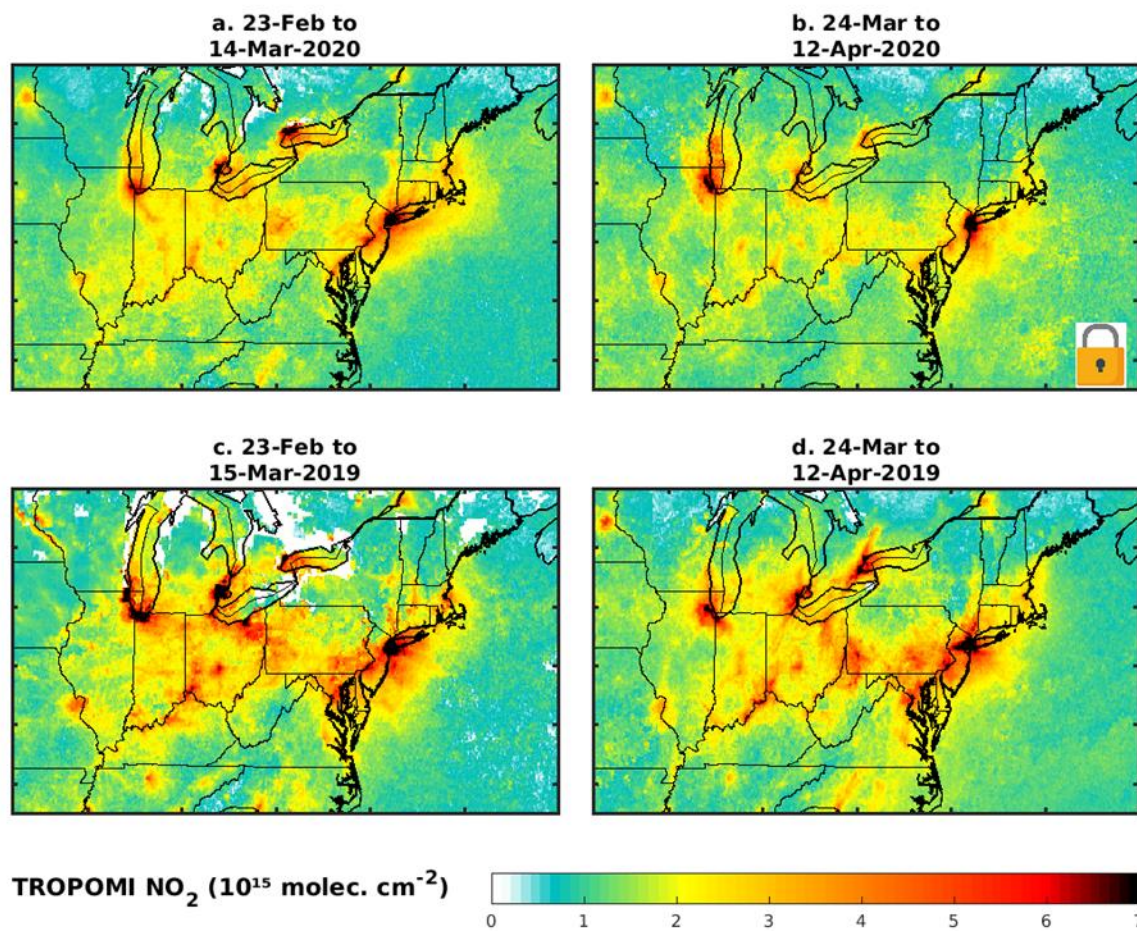
Figure 4. TROPOMI NO₂ columns over northeastern U.S. before and after the lockdowns in 2020 (a-b) and for the same periods in 2019 (c-d).

Table 1. NO$_2$ column reduction observed during the lockdown period, starting on the reference date and lasting 21 days, except for Iran where it lasts 17 days, relative to the same period in 2019. The averages are calculated using data within a 100 km radius around the city centers. The coordinates (latitude North and longitude East) are given. The lockdown period for China and Iran were chosen in order to eliminate interference of the national holidays. The uncertainties given within brackets are standard errors calculated from the retrieval uncertainties and accounting for the number of days with valid data.

City	lat	lon	Reference date	TROPOMI	OMI
Beijing	39.9	116.4	11-Feb-20	-25(±10)%	-33(±10)%
Chengdu	30.7	104.1	11-Feb-20	-19(±21)%	-10(±27)%
Chonqing	30.7	104.1	11-Feb-20	-43(±14)%	-11(±32)%
Dalian	38.9	121.6	11-Feb-20	-45(±8)%	-18(±16)%
Dongguan	23.0	113.7	11-Feb-20	-14(±16)%	-36(±11)%
Foshan	38.9	121.6	11-Feb-20	-34(±12)%	-51(±9)%
Guangzhou	23.1	113.3	11-Feb-20	-30(±14)%	-56(±8)%
Jinan	36.7	117.0	11-Feb-20	-69(±4)%	-63(±5)%
Nanjing	32.1	118.8	11-Feb-20	-49(±8)%	-57(±9)%
Qingdao	36.1	120.4	11-Feb-20	-54(±6)%	-43(±11)%
Shanghai	31.2	121.5	11-Feb-20	-11(±15)%	-29(±14)%
Shenyang	41.8	123.4	11-Feb-20	-52(±7)%	-29(±12)%
Tianjin	39.1	117.2	11-Feb-20	-46(±8)%	-37(±10)%
Wuhan	30.6	114.3	11-Feb-20	-43(±14)%	-57(±14)%
Xian	34.3	109.0	11-Feb-20	-56(±9)%	-57(±10)%
Zhengzhou	34.8	113.6	11-Feb-20	-53(±7)%	-64(±6)%
Milan	36.7	117	23-Feb-20	-38(±10)%	-24(±13)%
Venice	45.4	12.3	23-Feb-20	-33(±9)%	-33(±11)%
Madrid	40.4	-3.7	15-Mar-20	-29(±12)%	-21(±21)%
Barcelona	41.4	2.2	15-Mar-20	-32(±12)%	-31(±20)%
Paris	48.8	2.4	17-Mar-20	-28(±10)%	-28(±12)%
Brussels	50.9	4.4	17-Mar-20	-18(±11)%	-22(±11)%
Frankfurt	50.1	8.7	23-Mar-20	-21 (±11)%	-23(±13)%
Hamburg	53.6	10.0	23-Mar-20	-19(±12)%	-21(±15)%
Tehran	35.7	51.4	4-Mar-20	-27(±20)%	18(±19)%
Isfahan	32.7	51.7	4-Mar-20	37(±16)%	19(±19)%
Daegu	35.9	128.6	23-Feb-20	-24(±10)%	-34(±13)%
Seoul	37.6	127.0	23-Feb-20	-43(±7)%	-30(±10)%
New York	40.7	-73.9	24-Mar-20	-28(±11)%	-31(±14)%
Washington	38.9	-77.0	24-Mar-20	-21(±13)%	-12(±25)%
Philadelphia	39.9	-75.2	24-Mar-20	-24(±11)%	-11(±21)%
Chicago	41.9	-87.6	24-Mar-20	-19(±12)%	3(±25)%
Detroit	42.3	-83.0	24-Mar-20	-21(±12)%	-23(±21)%